ToxEHS

Arginine-rich Peptide Coated PLGA Nanoparticles Enhance Polymeric Delivery of Antisense HIF1α-oligonucleotide to Fully Differentiated Stiff Adipocytes

Da Hyeon Choi[1] **& Yoon Shin Park**[1]

[1]Major in Microbiology, School of Biological Sciences, College of Natural Sciences, Chungbuk National University, Cheongju 28644, Republic of Korea
Correspondence and requests for materials should be addressed to Y. S. Park (pys@cbnu.ac.kr)

Received 3 September 2018 / Received in revised form 16 December 2018
Accepted 26 December 2018
DOI 10.1007/s13530-019-0382-8

pISSN : 2005-9752 / eISSN : 2233-7784
Toxicol. Environ. Health. Sci. Vol. 11(1), 1-10, 2019

Abstract

Objective: The purpose of this study was developing the new delivery system of antisense HIF1α oligodeoxynucleotide (ASO) into the stiff adipocytes. As the adipogenesis progressed, accumulating lipid droplet in cytosol lead adipocytes membrane stiffness and difficulties in the delivery of therapeutic agents into the cytosol. Hypoxia affects a number of biological functions including angiogenesis, apoptosis, inflammation, and adipogenesis. Hypoxia-inducible transcription factor-1 alpha (HIF1α) is a major transcription factor that controls metabolic and adipogenic gene expression under hypoxia. Controlling HIFα expression can be a promising therapy for obesity treatment.
Methods: The ASO was synthesized and used in a complex with polylactic-*co*-glycolic acid (PLGA) nanoparticles (NP). To enhance the cell-penetrating capacity, the PLGA-ASO-NP complex was coated with arginine-rich peptide (ARP) in different N:P molar ratios (PLGA-ASO-NP:ARP = 1 : 1, 2 : 1, 5 : 1). To examine the intracellular and intranuclear delivery, these complexes were treated to fully differentiated adipocyte.
Results: The PLGA-ASO-NP/ARP improved the efficacy of ASO-delivery into stiff adipocytes by increasing the cell surface charge, determined by the zeta potential, and forming polyplexes with small particle size. The proper N:P molar ratio of PLGA-ASO-NP/ARP synthesis was 5:1 with significantly improved gene delivery efficiency and intracellular uptake in adipocytes. Furthermore, PLGA-ASO-NP/ARP was stable in serum for 8 h compared to naked ASO.
Conclusion: These results suggest that the PLGA-ASO-NP/ARP can provide an effective and serum-stable gene-delivery system, especially for cells with a stiff cell membrane.

Keywords: Arginine-rich peptide, Hypoxia-inducible transcription factor-1α, PLGA, Adipogenesis, Antisense oligonucleotide

Introduction

Obesity is a worldwide epidemic and a preventable leading cause of death with increasing prevalence both in adults and children[1]. It is one of the most severe public health problems of the 21st century[2]. Controlling obesity by inhibition of fat accumulation in adipocytes can cure various diseases including type 2 diabetes mellitus (T2DM), cancer, and cardiovascular complications, and it has received much attention and been the major subject of intensive research[1,2].

To treat obesity, a reduction of fat accumulation through various genetic modifications, including micro RNAs[3], siRNA[4], and antisense oligonucleotide agents[5], has been suggested. The FDA has approved antisense agents for clinical use[6], which implies the possibility of use in disease management. However, antisense agents are still limited in their clinical application because of their poor cell membrane permeability. Especially, increased stiffness of adipocytes with accumulation of lipid droplets during adipogenesis can decrease intracellular delivery of charged macromolecules such as antisense agents, resulting in low drug delivery efficacy[7,8]. In this context, overcoming the stiffness of adipocyte membranes is an important issue for obesity treatment. Therefore, improvement in the systemic and intracellular delivery of antisense agents is needed[9].

There have been efforts to enhance intracellular delivery of antisense agents using viral delivery systems[10], polymers[11,12], cell permeable peptides[13,14], or cationic

polymers[15] as carriers. Antisense agents have been widely accepted as a replacement for antibodies because of their target specificity and selectivity[16]. Antisense therapeutics is mostly focused on viral infections, wound healing, cardiovascular diseases, and cancer[17]. Only a few results have been reported on the application of antisense therapy for obesity[18,19] or hyperlipidemia[20,21] treatments. Several target genes have been reported as antisense oligonucleotide (ASO) agents for obesity and metabolic diseases, including nicotinamide N-methyltransferase (NNMT)-A, Fsp75, partial reduction of FSP27[19], IκB kinase β (IKKβ)[22], fibroblast growth factor receptor 4 (FGFR4)[23], beta-catenin[24], glucocorticoid receptor[25], and SREBP-1c[26].

Regardless of the frequent use of ASO for disease targeting and treatment, ASO therapy still has limitations due to poor cellular membrane permeability because of the negatively charged macromolecules and low serum stability[27]. To overcome these issues, polymers such as polylactic-*co*-glycolic acid (PLGA) and polyethyleneimine (PEI)[3,28,29] have been suggested. We previously reported the anti-obesity effect of ASO-HIF1α conjugated with the cell permeable peptide low molecular weight protamine, LMWP[27]. The HIF1α, hypoxia-inducible factor-1α, is a key transcription factor that regulates the expression of numerous genes related to angiogenesis, metabolism, and cell cycle under a hypoxic environment[30]. Especially, hypoxia might be a strong modulator of angiogenesis associated with adipose tissue expansion and fat accumulation. In this regard, HIF1α could be a master regulator that controls angiogenesis as well as adipogenesis. A recent clinical study revealed that HIF1α expression is elevated in obese subjects and decreases following weight loss[31]. Therefore, targeting and suppression of the HIF1α gene with elevated cell-penetrating capacity and serum stability could be a promising strategy for treatment of obesity.

In our previous report, the chemical conjugates of ASO-HIF1α with CPP provided similar cell penetration capacity with the liposomal delivery agent, Lipofectamine, and stability in a DNase I- and GSH-containing environment[27]. Hence, we need to enhance serum stability and cell permeability for future clinical applications. Nanoparticle (NP) gene-delivery systems have received attention and been extensively investigated due to their desirable properties[32,33]. Especially, an NP gene-delivery system with a hydrophilic cell surface structure can effectively prevent aggregation of NP and ensure a longer circulation time in the blood[3].

Polyactic-*co*-glycolic acid (PLGA) NP was initially used to encapsulate genetic-based therapeutics after they demonstrated endo-lysosomal escape characteristics, while being biodegradable and cell-compatible. However, the structure of nucleic acid molecules is likely degraded during sphere preparation. In addition, the negative zeta potential of PLGA-NP interrupts the cellular uptake of NP, decreasing the cellular delivery efficacy. To solve this issue, conjugation of PLGA-NP with cell-penetrating peptides (CPP) has been suggested.

Various types of arginine-rich peptides (ARP) that possess very similar characteristics to those of CPP in terms of translocation and as a delivery vector have been reported[34]. The CPP have been used widely for intracellular delivery of various macromolecules and nanostructured systems. We previously reported the development of low molecular weight protamine (LMWP) as an effective yet nontoxic CPP[35] or membrane translocalization carrier[36]. Both *in vitro* and *in vivo* investigations have demonstrated that LMWP was able to translocate its attached protein, gene, or carrier cargo into various types of cells[36].

Here, with the objective of promoting PLGA-NP as a gene carrier, we synthesized an ARP peptide with hydrophobic chains anchoring into a polylactic-*co*-glycolic acid (PLGA) nanoparticle (NP) with ASO-HIF1α and then modified its surface with ARP to enhance target cell association and internalization. We investigated the ability of ASO-HIF1α-PLGA/ARP to increase intracellular and intranuclear delivery efficacy with little cytotoxicity and increased serum stability.

Results

Particle Size and Zeta Potential of PLGA-ASO-NP

The whole scheme for synthesis of the PLGA-ASO-NP/ARP is depicted in Figure 1. The mean particle diameter and zeta-potential of PLGA/PEI/CTAB-nanoparticles (PLGA-NP) and its complex with PLGA-ASO-NP were measured. The PLGA-NP was first formulated from 1.67 wt% PLGA, 0.83% cationic material (PEI and CTAB), and 2.23% mannitol. The mean particle diameter of PLGA-NP was approximately 155.9 ± 6.0 nm. In complex formation with antisense oligonucleotide-HIF1α (ASO), PLGA-ASO-NP showed larger particle diameters (268.3 ± 17.7 nm), possibly due to agglomeration of particles by compression (Table 1). The zeta potential of the PLGA-NP itself was 35.3 ± 0.9 mV, which decreased to 19.5 ± 2.3 mV through complex formation with ASO.

Gel Retardation Assay of PLGA-ASO-NP

Complex formation of PLGA-NP with ASO was assessed by agarose gel electrophoresis. To form PLGA-ASO-NP, different concentrations of ASO-HIF1α (0.1, 5, 10, 50, 100, 200, 500, and 1000 mM) were added to

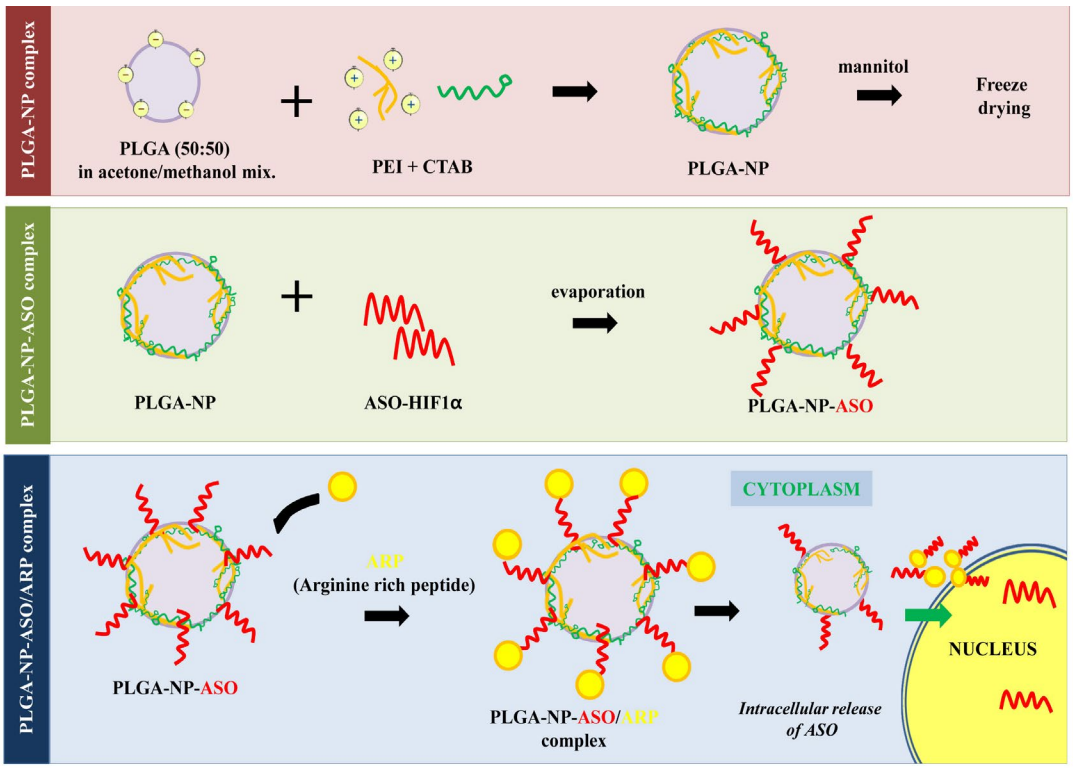

Figure 1. An illustrated scheme of this experiment. PLGA: polylactic-*co*-glycolic acid, PEI: polyethylene imine, CTAB: cetrimonium bromide, ASO: antisense HIF1α oligonucleotide, ARP: arginine-rich protein.

Table 1. Characteristics of PLGA-ASO-NP and ARP-modified PLGA-ASO-NP. The mean particle diameter and zeta-potential of PLGA/PEI/CTAB-nanoparticles (PLGA-NP) and its complex with PLGA-ASO-NP were measured. The mean particle diameter of PLGA-NP was significantly increased. The zeta potential of the complex of ASO with PLGA-NP was decreased. The size of PLGA-ASO-NP/ARP was decreased with increasing ARP binding molar ratio. Hence, the zeta potential was increased. It indicates that the PLGA-ASO-NP/ARP is a favorable agent for cell penetration. Statistical significance was analyzed using the Student's *t*-test. Different letters (a, b, and c) indicate statistically significant differences among groups ($P < 0.05$).

	Size (nm)	Z-potential (mV)
PLGA-NP	155.9 ± 6.0	35.3 ± 0.9
PLGA-NP-ASO	268.3 ± 17.7*	19.5 ± 2.3*
PLGA-NP-ASO : ARP (N:P = 1:1)	289.3 ± 12.0[a]	33.4 ± 3.9[a]
PLGA-NP-ASO : ARP (N:P = 2:1)	178.0 ± 3.0[b]	43.1 ± 2.1[b]
PLGA-NP-ASO : ARP (N:P = 5:1)	158.9 ± 2.7[c]	51.4 ± 0.6[c]

PLGA solution (1 mg/mL). Naked ASO was used as a control. As shown in Figure 2A, naked ASO migrated downward rapidly. Stable PLGA-ASO-NP complex was maintained to 100 mM of ASO. Migration of the PLGA-ASO-NP complex was observed from 100 mM HIF1α (Figure 2A). Hence, according to the serum stability assay, the maximum concentration of ASO for PLGA-ASO-NP complex was determined to be 50 mM based on analysis of various concentrations of ASO-containing PLGA nanocomplexes (0.1, 1, 5, 10, 50, 100, 200, 500, and 1000 mM) incubated in 50% FBS solution for 4 h. Naked ASO-HIF1α was used as a control and migrated downward rapidly. No migration was observed with 50 mM of antisense HIF1α (Figure 2B). In contrast, migration of the PLGA-ASO-NP complex was observed from 100 mM of HIF1α concentration (Figure 2B). According to the gel retardation and serum stability assay, 50 mM of ASO was the optimal concentration for PLGA-ASO-NP complex formation.

Characteristics of PLGA-ASO-NP/ARP

Two of the most important parameters of a gene-carrier, zeta potential and particle size, were investigated by dynamic light scattering (Table 1). The PLGA-

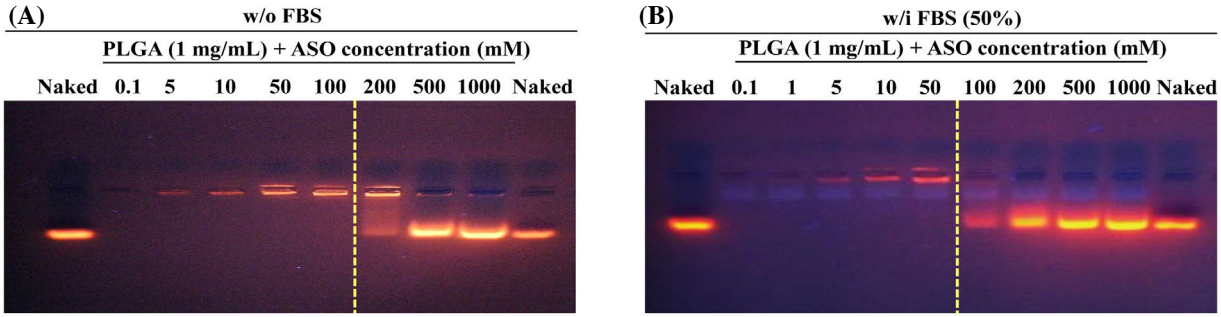

Figure 2. Gel retardation and serum stability assay of the ASO-PLGA-NP complex. To determine the optimum concentration of ASO for PLGA-ASO-NP/ARP complexes, (A) the PLGA-NP was mixed with varying concentrations of ASO to form PLGA-ASO-NP, and the samples were analyzed by gel retardation assay using an agarose gel electrophoresis. (B) Then PLGA-ASO-NP was incubated in media containing 50% FBS to examine the serum stability.

ASO-NP was modified with ARP with varying N:P molar ratio (1:1, 2:1, and 5:1). The zeta potential of PLGA-ASO-NP/ARP increased from 33.4 ± 3.9 mV to 51.4 ± 0.6 mV, and particle size decreased from 289.3 ± 12.0 nm to 158.9 ± 2.7 nm as the N:P molar ratio increased, indicating the PLGA-ASO-NP/ARP is a favorable agent for cell penetration.

Cytotoxicity of PLGA-ASO-NP/ARP

To assess the cell viability of PLGA-ASO-NP/ARP, we conducted an MTT assay.

Although ARP has been demonstrated to be safe and non-toxic[35], we need to evaluate the cytotoxicity of the nanoparticle. For this purpose, we used an MTT assay to examine the effect of the PLGA nanoparticles containing the optimal concentration of 50 mM ASO on cytotoxicity. As shown in Figure 3, PLGA-ASO-NP/ARP-treated 3T3-L1 preadipocytes yielded little cell cytotoxicity at varying N : P ratios of ARP.

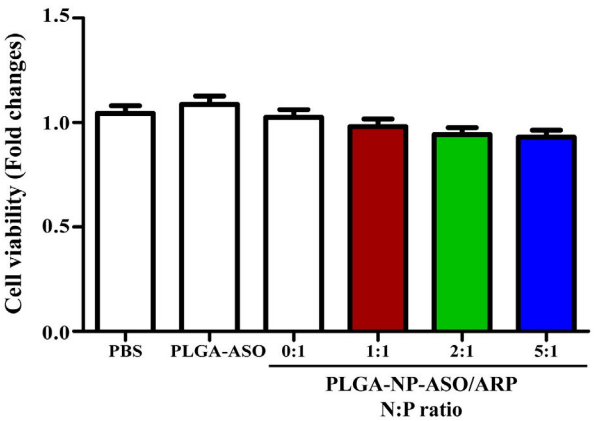

Figure 3. Cytotoxicity of PLGA-ASO-NP/ARP. To assess cytotoxicity of PLGA-ASO-NP/ARP, an MTT assay was conducted. The ASO concentration used for PLGA-ASO-NP/ARP formation was 50 mM, which was determined by the gel retardation assay presented in Figure 2.

Intracellular and Intranuclear Uptake of PLGA-ASO-NP/ARP

The cellular uptake and intracellular localization of the PLGA-ASO-NP/ARP were analyzed in 3T3-L1 cells using confocal microscopy (Figure 4). We used fully differentiated 3T3-L1 cells to examine the intracellular delivery efficacy of PLGA-ASO-NP/ARP. As shown in Figure 4A, the cytosol of fully adipogenic differentiated 3T3-L1 cells was mostly filled with lipid droplets, which created the cell membrane stiffness. Differentiated 3T3-L1 cells were detached with trypsin and re-seeded to investigate the delivery efficacy of PLGA-ASO-NP/ARP into the stiff cells. Little cell penetration was observed in 3T3-L1 cells treated with PLGA-ASO-NP only (Figure 4B). However, the apparent capacity for penetration into the cell and even the nuclei of the cells were seen in treated PLGA-ASO-NP/ARP cells as the N:P molar ratio increased. Especially, the complex with the N:P ratio 5:1 showed the best intracellular and intranuclear uptake capacity.

DNase I Stability of the PLGA-ASO-NP/ARP

We also examined the stability of the PLGA-ASO-NP/ARP against nuclease degradation. DNase I (50 units) was added to PLGA-ASO-NP/ARP containing different molar ratios of ARP (N:P = 1:5), followed by incubation of the reaction mixture for various time periods (0, 0.5, 1, 2, 4, 8, 12, 24, and 48 h) at 37°C. The PLGA-ASO-NP/ARP was stable for 8 h, indicating that the complex with ARP resulted in protection of PLGA-ASO-NP against nuclease digestion (Figure 5A).

Serum Stability of PLGA-ASO-NP/ARP

To further apply this complex to the cells, we investigated the serum stability of PLGA-ASO-NP/ARP com-

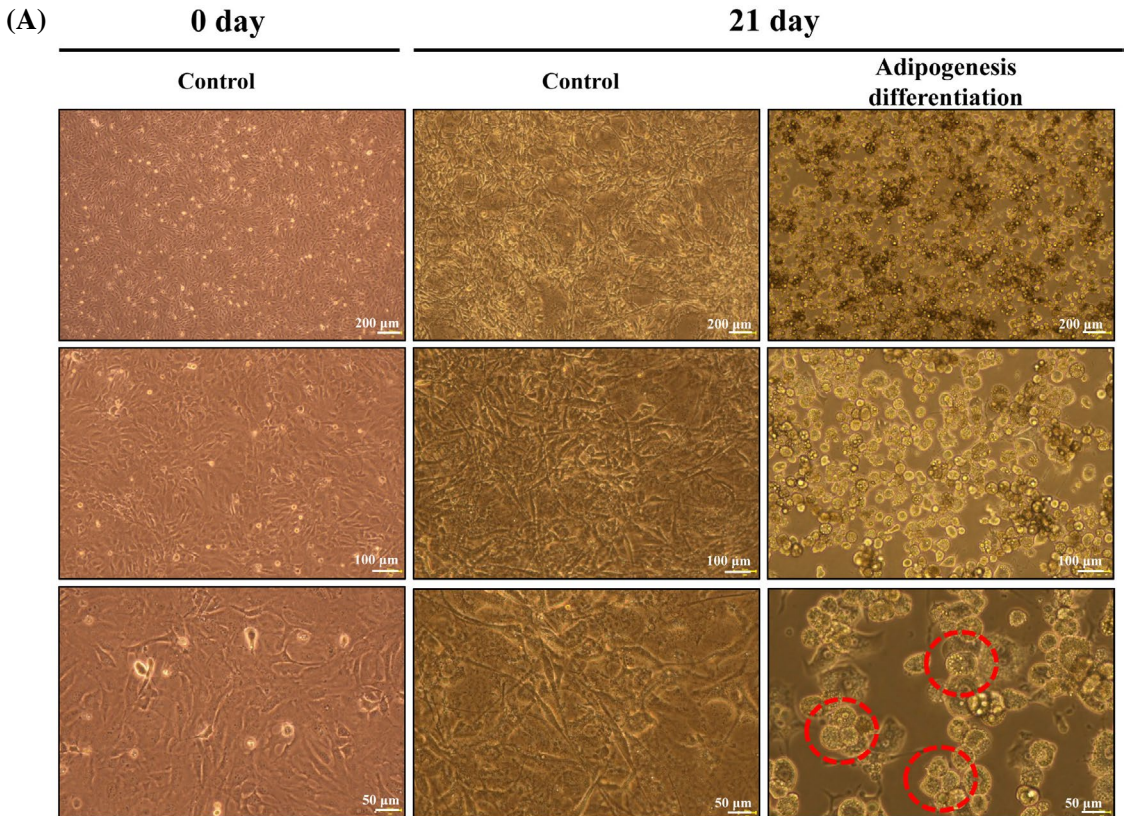

Figure 4. Intracellular and intranuclear uptake of PLGA-ASO-NP/ARP. Cellular uptake and intracellular localization of PLGA-ASO-NP/ARP were conducted with fully differentiated 3T3-L1 cells and analyzed using confocal microscopy. (A) The 3T3-L1 preadipocytes were differentiated into adipocytes by incubation with adipogenic media for 3 weeks. With the differentiation process, the accumulation of lipid droplet in cytosol was significantly increased and it was marked with a red dotted circle. (B) To examine the intracellular delivery of PLGA-ASO-NP/ARP, differentiated adipocytes were detached, reseeded onto the coverslip, and treated with varying N:P molar ratios of PLGA-ASO-NP/ARP. Apparent cell penetration capacity and nuclear penetration were seen with PLGA-ASO-NP/ARP (N:P = 5:1).

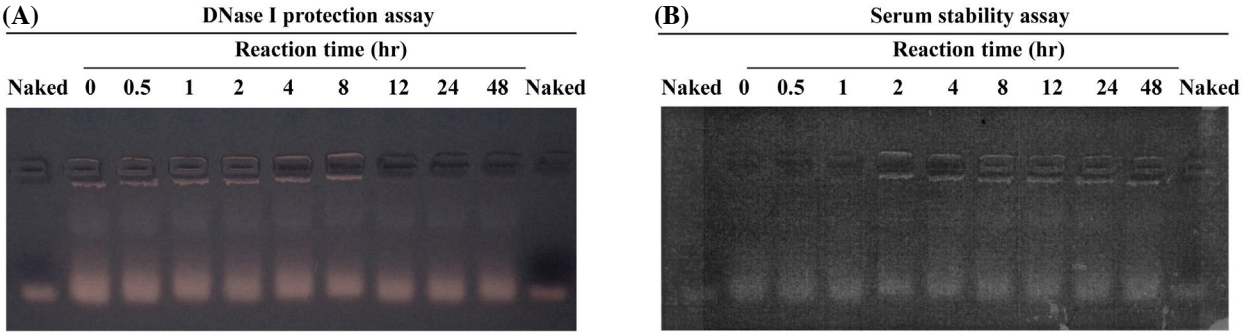

Figure 5. PLGA-ASO-NP/ARP stability against DNase I and serum. To investigate the DNase I protective effect and serum stability of PLGA-ASO-NP/ARP complexes, we incubated in DNase I and 50% FBS-containing media, respectively. (A) The DNase I protection and (B) serum stability of PLGA-ASO-NP/ARP were evaluated using an agarose gel retardation method.

plex by incubating the complex in 50% FBS solution for indicated time points (0, 0.5, 1, 2, 4, 8, 12, 24, and 48 h). Naked antisense HIF1α, used as a control, migrated downward rapidly. However, no migration of HIF1α gene was observed until 48 h (Figure 5B). According to the DNase I and serum stability assay, the ASO-PLGA-NP/ARP complex can be stable and maintain its activity at least for 8 h.

Discussion

The aim of this study was to develop a cell permeable polymeric nanoparticle for improving targeted gene delivery into stiff adipocytes. Despite all the efforts to understand the pathophysiology related to obesity, drug development for obesity therapy is lagging. The various functions of adipose tissue in different diseases such as obesity, type 2 diabetes, and cardiovascular complications have become the subject of intensive research[2]. For further investigation of molecular mechanisms and pathways underlying the complex biology of adipose tissue, access to genetic tools is essential to design cell permeable NP that improve cell binding capacity and direct cell membrane penetration into fat-containing adipocytes is crucial to achieve therapeutic efficacy in drug and gene delivery. Here, we developed PLGA-ASO-NP/ARP to improve the intracellular delivery of ASO-HIF1α into fully differentiated adipocytes. We modified the surface of PLGA-ASO-NP with ARP to increase NP internalization and found that this modified complex significantly increased intracellular and intranuclear delivery of ASO-HIF1α with little cytotoxicity. Using ASO as a cell therapeutic agent is important because it has similar targeting efficacy to antibodies through target cell selectivity and internalization into the cells by endocytosis[16].

The optimization of PLGA-ASO-NP for cell penetration with little cytotoxicity is challenging because the cell-NP interaction is very complex depending on the surface-modification, size, and characteristics of the cells[37,38]. The size and zeta potential of PLGA-ASO-NP influence their stability as well as their interaction with negatively charged cell membranes[29], which is the critical step for successful intracellular uptake, especially for cells with a stiff membrane[39]. One way of functional groups on the PLGA-ASO-NP surface can influence cell-NP interactions is by modulating the N:P surface charge. Therefore, we prepared PLGA-ASONP complex with ARP at varying N:P molar ratios. As reported previously[3], NP shows low transfection efficiency as the N:P ratio decreases. This implies that the low zeta potential of NP does not easily react with negatively charged cell surfaces, making ASO delivery difficult.

As described in Figure 4, positively-charged NP complexes with ARP showed the greatest cell internalization efficiency because of strong electrostatic interactions with negatively-charged moieties on the cell surface, as shown in previous reports[40-42]. In addition to charge and hydrophobicity, the size of the PLGA-ASO-NP/ARP can affect internalization and cellular trafficking. As the N:P molar ratios increases, the mean size of the PLGA-ASO-NP/ARP complex decreased (from 289.3 to 158.9 nm), indicating that the complexes were nano-sized structures (100-200 nm) for favorable intracellular drug penetration[43].

The cytotoxicity of the complex is based on the concentration or N:P molar ratio of ARP for complex formation. As expected, PLGA-ASO-NP/ARP did not show any detectable cytotoxic effect (Figure 3). Hence, we observed cell toxicity at an N:P ratio over 1: 10 (data not shown).

Another important factor for delivery of ASO is maintenance of its biological activity and stability[44]. Protection of ASO from degradation by DNase I for up to 8 h was detected for the complex, indicating that the com-

plex formation of ASO with PLGA-NP with ARP protects ASO against DNase I reaction. Although the mechanism of this protective effect is not solved yet, this characteristic is of great importance for any possible future *in vivo* and clinical application. The current results are in good agreement with other studies in which the positively-charged surface modifications to PLGA-NP with CPP produced higher uptake than that of negatively-charged NP[45-48].

Conclusion

The current study provides effective intracellular delivery system of therapeutic target genes for the cells with stiff membrane. Using the cell permeable peptide ARP, we successfully designed ASO-HIF1α complex with PLGA-NP and demonstrated that cell permeable polymeric ASO-HIF1α may provide a novel strategy for anti-obesity drug development. Importantly, designed polymeric NP showed effective cell penetration capacity even to fully differentiated fat-containing adipocytes. Furthermore, we demonstrated that it is safe for the cells and stable in serum. This complex may potentially be applicable for treatment of obese patients.

Materials and Methods

Materials

Acetone, methanol, PEI (branched, ~13 kDa), cetrimonium bromide (CTAB), mannitol, 3-[4,5-dimethylthiazol-2-yl]-2,5-diphenyltetrazolium bromide (MTT), and DNase I were purchased from Sigma-Aldrich Co. (St. Louis, MO, USA). D, L-Lactide/glycolide copolymer (PLGA, ester terminated, lactic : glycolic molar ratio 50 : 50, molecular weight [MW] 30 kDa) was purchased from LACTEL Absorbance Polymers (Birmingham, AL). Fetal bovine serum (FBS), phosphate-buffered saline (PBS), 0.25% (w/v) trypsin-EDTA, Dulbecco's modified essential medium (DMEM), Dulbecco's phosphate-buffered saline (PBS), penicillin-streptomycin, Lipofectamine 2000, and 4′, 6-diamidino-2-phenylindole (DAPI) were purchased from Gibco-BRL (Invitrogen, Carlsbad, CA). Heparin and desalting columns were obtained from GE Healthcare (Piscataway, NJ). The 3T3-L1 pre-adipocytes were purchased from American Type Culture Collection (ATCC, Manassas, VA, USA). The sequences of antisense oligonucleotide (ASO)-hypoxia inducible factor-1α (HIF1α) and 6-fluorescein amidite (6-FAM)-labeled ASO were chemically synthesized by Integrated DNA Technologies, Inc. (Skokie, IL) as follows: 5′-ACA ACG CGG GCA CCG ATT CGC CAT G-3′ for ASO. Other reagents of analytical grade were obtained from suppliers and used without purification. Unless otherwise noted, all chemicals and reagents were analytical grade and obtained from Sigma (St. Louis, MO).

Preparation of the ARP

The ARP was prepared in mass quantities using a peptide synthesizer (Apex 396; AAPPTec, Louisville, KY, USA). The synthesized ARP was purified by reverse-phase high-performance liquid chromatography with a Vydac C18 column and a gradient of water/acetonitrile containing 0.1% TFA. The purity of the synthesized ARP was above 98%.

Preparation of PLGA Nanoparticles

The PLGA nanoparticles were prepared by the oil-in-water emulsion solvent-evaporation method, as reported previously, with some modification[28].

The acetone/methanol mixture (2:1, 12 mL) containing PLGA (200 mg) was completely melted by vigorous vortexing. In a separate tube, the CTAB (100 mg) was added to PEI (400 mg), and the mixture was added to PLGA solution drop by drop. The cationic PLGA/CTAB/PEI was added into 100 mL of DW and stirred for 1 h at room temperature. Mannitol (2.5 g) was added to the stirred cationic PLGA solution, and the solution was stirred for another 1 h. The PLGA polymer solution containing mannitol was centrifuged at 14,000 RPM at 4°C for 15 min. The supernatant was collected and freeze-dried (Ilshin BioBase, Gyeong-gi, Korea) for further analysis. The PLGA nanoparticles containing cationic materials dispersed in mannitol were obtained by freeze-drying.

Preparation of Cationic PLGA Nanoparticle Complex with ASO

The cationic PLGA nanoparticles (PLGA-NP) for antisense-HIF1α oligonucleotide (ASO) nanoparticle complexes were formulated by adding varying concentrations of ASO (0, 5, 10, 50, 100, 200, 500, and 1000 μM) into the PLGA nanoparticles (1 mg/mL). Then the complex was agitated at 4°C for 16 h. The optimal concentration of ASO for stable and effective complex formation with cationic PLGA nanoparticles was determined by gel retardation assay, serum stability assay and DNase I stability assay.

Preparation of ARP-modified PLGA-NP

The PLGA-NP/ARP charge ratio (nitrogen:phosphate [N:P]) is expressed as the mole ratio of the amine groups of ARP to the phosphate of ASO. The complexes were self-assembled in PBS buffer (150 mM, pH 7.4) by mixing the ASO with the PLGA solution at varying charge ratios (N:P = 1:1, 2:1, and 5:1), keeping the

amount of ASO constant. The complexes were incubated for 30 min at room temperature.

Measurements of Particle Size and Zeta Potential

The particle size and zeta potential (surface charge) of each NP sample formed at various N:P ratios were determined at 25°C with a scattering angle of 90° by a Zetasizer (Malvern, UK). The PLGA-ASO-NP/ARP complexes were prepared in PBS and diluted with deionized water to ensure that the evaluations were conducted under low ionic strength conditions, where the surface charge of the particles can be accurately determined.

DNase I Protection Assay

The DNase I protection assay was conducted using a slightly modified procedure from a previous report[27]. Briefly, the cationic PLGA-NP and its complex with ARP were employed in the preparation of PLGA nanoparticle complex. The DNase I (50 units) was added to the solution of PLGA-ASO-NP compounds, and mixed solutions were incubated for varying time points (0, 0.5, 1, 2, 4, 8, 12, 24, and 48 h) at 37°C. During incubation, 50 μL of each suspension was withdrawn at different time points, mixed with 75 μL of the quenching solution (4 M ammonium acetate, 20 mM EDTA, and 2 mg/mL glycogen), and then placed on ice. Then, the ASO was dissociated from ARP by addition of 1.0% SDS (37 μL) to the suspension, and the mixture was heated overnight at 65°C. The ASO was precipitated and extracted after incubation by treating the suspension with phenol/chloroform (1:1, v/v), and then the precipitate was treated with ethanol to extract the ASO. The ASO pellet was then dissolved in 10 μL TE buffer and applied to 1% agarose gel electrophoresis. Naked ASO was used as the control and treated with the same procedure.

Serum Stability of PLGA-ASO-NP/ARP

Serum stability of PLGA-ASO-NP/ARP complex was investigated by incubating the complex (100 μL) in FBS solution (100 μL, 50% FBS) for indicated time points (0, 0.5, 1, 2, 4, 8, 12, 24, and 48 h) at room temperature. The incubated complex solutions were applied to 1% agarose gel electrophoresis. Naked antisense HIF1α was used as a control.

Preadipocyte Culture and Cell Viability

The 3T3-L1 pre-adipocyte cell line was cultured in DMEM supplemented with 10% heat-inactivated FBS at 37°C in a humidified atmosphere of 5% CO_2. Cell viability was evaluated by an MTT assay. Cells were seeded in 96-well plates at a density of 6×10^3 cells per well with DMEM culture medium with 10% FBS and 1% antibiotic and cultured for 24 h before testing. Cells were incubated with the PLGA/ARP NP for 48 h. An MTT (20 μL, 5 mg/mL) solution was added to each well and incubated with cells for another 4 h. After removal of the medium, 200 μL DMSO was added to each well, and the absorbance was measured at 490 nm using a microplate reader (Multiskan, Thermo Fisher, USA). The percent cell viability was measured as follows[27]:

$$\text{Cell viability (\%)} = [\text{Abs570 (sample)}] / [\text{Abs570 (control)}] \times 100$$

Adipocyte Differentiation Following Treatment with the PLGA-ASO-NP/ARP

Adipocyte differentiation was conducted as previously described[27]. In brief, 3T3-L1 preadipocytes were seeded into a 6-well plate (3×10^5 cells/well), cultured in DMEM supplemented with 10% FBS, and maintained in a 37°C incubator. When the cells reached 90% confluency, differentiation was induced by changing to adipogenic differentiation medium containing 0.5 mM 3-isobutyl-1-methyxanthine (IBMX), 10 μg/mL insulin, and 0.25 μM dexamethasone (DEX) for 3 weeks. Adipogenic medium was changed every 3 days. Cell differentiation was then assessed from the morphological changes[27]. The drug components, PLGA-ASO-NP only, and the PLGA-ASO-NP/ARP complex with various N:P ratios (N:P = 1:1, 2:1, and 5:1) were applied to induce differentiation into adipocytes. Before treatment, fully differentiated cells were detached with trypsin and reattached to the coverslip for confocal microscopy to clearly identify the cell morphology. Transfection of ASO using Lipofectamine was conducted in a 6-well plate when the cells reached about 60-70% confluence, following the manufacture's protocol. After transfection, FBS-containing growth medium was added to each well, and cells were incubated overnight and then examined to determine the ASO delivery efficacy. ASO delivery with Lipofectamine was used as a positive control.

Intracellular and Intra-nuclear Delivery of the PLGA-NP/ARP

The complex-treated differentiated 3T3-L1 cells were incubated in DMEM culture medium containing 10% FBS and 1% antibiotic at 37°C with 5% CO_2. Cells were maintained on coverslips in a 24-well plate for 24 h. The PLGA-NP and PLGA-NP/ARP were added and incubated with cells in the complete culture medium for 4 h. The ASO was tagged with 6-FAM. Fluorescence images were obtained by fluorescence microscopy (OLYMPUS IX-70). For intranuclear distribution study, DAPI was used for the nucleus staining, and the stained images were processed using confocal laser scanning microscopy (CLSM) (Olympus FV1000, Japan).

Cell Cytotoxicity (MTT) Assay and Proliferation Assay

The cytotoxicity was determined using a 3-(4,5-dimethylthiazol-2-yl)-2,5-diphenyl-2H-tetrazolium bromide (MTT) conversion assay[49]. Briefly, after seeding 3T3-L1 cells in a 96-well plate, cells were incubated with varying concentrations (0, 0.5, 1.0, 1.5, 2, 5, and 10 μg/mL) of ASO for 24 h at 37°C. Then, 100 μL aliquots solution containing MTT (5 mg/mL in complete DMEM) were added, followed by an additional 5 h incubation. The MTT-containing medium was removed, and dimethyl sulfoxide (DMSO, 200 μL) was added to dissolve the formazan crystals formed by live cells. Absorbance at 570 nm was measured, and the cell viability (%) was calculated according to the following equation:

$$\text{Cell viability}\,(\%) = [\text{OD570 (sample)}/\text{OD570 (control)}] \times 100.$$

The number of viable cells after treatment with the test compounds was measured using a hemocytometer. Test groups for cellular MTT and proliferation studies were: 1) PLGA-NP alone and 2) PLGA-NP/ARP treatment groups with varying N:P ratio (0:1, 1:1, 2:1, and 5:1).

Statistical Analysis

Statistical analysis was performed using the SPSS (Version 21.0) program (International Business Machines Corporation). All data are expressed as mean ± SD. Statistical significance was analyzed using the Student's *t*-test. The level of significance is represented as $*P < 0.05$. Statistically significant difference among groups was assessed using one-way ANOVA. One-way ANO VA was followed by the Tukey analysis as a *post hoc* analysis ($P < 0.05$). Different letters indicate statistically significant differences.

Acknowledgements

This study was supported by the Basic Science Research Program through the National Research Foundation of Korea (NRF) funded by the Ministry of Science, ICT & Future Planning (2017R1A2B4002611), and partly by the Technological innovation R&D program of SMBA (S2449311).

Conflict of Interest

The authors declare that they have no financial conflicts of interest with the contents of this article.

References

1. Barness, L. A., Opitz, J. M. & Gilbert-Barness, E. Obesity: genetic, molecular, and environmental aspects. *Am. J. Med. Genet. A.* **143A**, 3016-3034 (2007).
2. Hjartaker, A., Langseth, H. & Weiderpass, E. Obesity and diabetes epidemics: cancer repercussions. *Adv. Exp. Med. Biol.* **630**, 72-93 (2008).
3. Zhu, Y. *et al*. A novel type of self-assembled nanoparticles as targeted gene carriers: an application for plasmid DNA and antimicroRNA oligonucleotide delivery. *Int. J. Nanomedicine* **11**, 399-410 (2016).
4. Mykhaylyk, O. *et al*. Magnetic nanoparticle and magnetic field assisted siRNA delivery in vitro. *Methods. Mol. Biol.* **1218**, 53-106 (2015).
5. Le, T. D., Nakagawa, O., Fisher, M., Juliano, R. L. & Yoo, H. RGD Conjugated Dendritic Polylysine for Cellular Delivery of Antisense Oligonucleotide. *J. Nanoc.* **17**, 2353-2357 (2017).
6. Jabs, D. A. & Griffiths, P. D. Fomivirsen for the treatment of cytomegalovirus retinitis. *Am. J. Ophthalmol.* **133**, 552-556 (2002).
7. Shoham, N. *et al*. Adipocyte stiffness increases with accumulation of lipid droplets. *Biophys. J.* **106**, 1421-1431 (2014).
8. Zhang, C. & Liu, P. The lipid droplet: A conserved cellular organelle. *Protein & Cell* **8**, 796-800 (2017).
9. Garcia-Chaumont, C., Seksek, O., Grzybowska, J., Borowski, E. & Bolard, J. Delivery systems for antisense oligonucleotides. *Pharmacol. Ther.* **87**, 255-277 (2000).
10. Gao, J. Q. *et al*. Effective tumor targeted gene transfer using PEGylated adenovirus vector via systemic administration. *J. Control. Release*. **122**, 102-110 (2007).
11. Park, K. Non-ionic polymersomes for delivery of oligonucleotides. *J. Control. Release*. **134**, 73 (2009).
12. Kim, Y. *et al*. Polymersome delivery of siRNA and antisense oligonucleotides. *J. Control. Release*. **134**, 132-140 (2009).
13. McClorey, G. & Banerjee, S. Cell-Penetrating Peptides to Enhance Delivery of Oligonucleotide-Based Therapeutics. *Biomedicines* **6** (2018).
14. Astriab-Fisher, A., Sergueev, D., Fisher, M., Shaw, B. R. & Juliano, R. L. Conjugates of antisense oligonucleotides with the Tat and antennapedia cell-penetrating peptides: effects on cellular uptake, binding to target sequences, and biologic actions. *Pharm. Res.* **19**, 744-754 (2002).
15. Dong, L. *et al*. Targeting delivery oligonucleotide into macrophages by cationic polysaccharide from Bletilla striata successfully inhibited the expression of TNF-alpha. *J. Control. Release*. **134**, 214-220 (2009).
16. Fisher, A. A. *et al*. Evaluating the specificity of antisense oligonucleotide conjugates. A DNA array analysis. *J. Biol. Chem.* **277**, 22980-22984 (2002).
17. Luten, J., van Nostrum, C. F., De Smedt, S. C. & Hennink, W. E. Biodegradable polymers as non-viral carriers for plasmid DNA delivery. *J. Control. Release*. **126**, 97-110 (2008).
18. Ropelle, E. R. *et al*. Inhibition of hypothalamic Foxo1 expression reduced food intake in diet-induced obesity rats. *J. Phtsiol.* **587**, 2341-2351 (2009).
19. Langhi, C. *et al*. Therapeutic silencing of fat-specific

protein 27 improves glycemic control in mouse models of obesity and insulin resistance. *J. Lipid. Res.* **58**, 81-91 (2017).
20. Cao, Y. *et al*. Antisense oligonucleotide and thyroid hormone conjugates for obesity treatment. *Sci. Rep.* **7**, 9307 (2017).
21. Crooke, R. M. *et al*. An apolipoprotein B antisense oligonucleotide lowers LDL cholesterol in hyperlipidemic mice without causing hepatic steatosis. *J. Lipid. Res.* **46**, 872-884 (2005).
22. Helsley, R. N. *et al*. Targeting IkappaB kinase beta in Adipocyte Lineage Cells for Treatment of Obesity and Metabolic Dysfunctions. *Stem Cells* **34**, 1883-1895 (2016).
23. Yu, X. X. *et al*. Peripheral reduction of FGFR4 with antisense oligonucleotides increases metabolic rate and lowers adiposity in diet-induced obese mice. *PLoS One* **8**, e66923 (2013).
24. Popov, V. B. *et al*. Second-generation antisense oligonucleotides against beta-catenin protect mice against diet-induced hepatic steatosis and hepatic and peripheral insulin resistance. *FASEB. J.* **30**, 1207-1217 (2016).
25. Watts, L. M. *et al*. Reduction of hepatic and adipose tissue glucocorticoid receptor expression with antisense oligonucleotides improves hyperglycemia and hyperlipidemia in diabetic rodents without causing systemic glucocorticoid antagonism. *Diabetes* **54**, 1846-1853 (2005).
26. Vitto, M. F. *et al*. Reversion of steatosis by SREBP-1c antisense oligonucleotide did not improve hepatic insulin action in diet-induced obesity mice. *Horm. Metab. Res.* **44**, 885-890 (2012).
27. Park, Y. S. *et al*. Specific down regulation of 3T3-L1 adipocyte differentiation by cell-permeable antisense HIF1alpha-oligonucleotide. *J. Control. Release.* **144**, 82-90 (2010).
28. Takashima, Y. *et al*. Spray-drying preparation of microparticles containing cationic PLGA nanospheres as gene carriers for avoiding aggregation of nanospheres. *Int. J. Pharm.* **343**, 262-269 (2007).
29. Kolte, A., Patil, S., Lesimple, P., Hanrahan, J. W. & Misra, A. PEGylated composite nanoparticles of PLGA and polyethylenimine for safe and efficient delivery of pDNA to lungs. *Int. J. Pharm.* **524**, 382-396 (2017).
30. Hosogai, N. *et al*. Adipose tissue hypoxia in obesity and its impact on adipocytokine dysregulation. *Diabetes* **56**, 901-911 (2007).
31. Fleischmann, E. *et al*. Tissue oxygenation in obese and non-obese patients during laparoscopy. *Obes. Surg.* **15**, 813-819 (2005).
32. Malcolm, D. W., Varghese, J. J., Sorrells, J. E., Ovitt, C. E. & Benoit, D. S. W. The Effects of Biological Fluids on Colloidal Stability and siRNA Delivery of a pH-Responsive Micellar Nanoparticle Delivery System. *ACS. nano.* **12**, 187-197 (2018).
33. Yang, C. *et al*. Theranostic poly (lactic-co-glycolic acid) nanoparticle for magnetic resonance/infrared fluorescence bimodal imaging and efficient siRNA delivery to macrophages and its evaluation in a kidney injury model. *Nanomedicine* **13**, 2451-2462 (2017).
34. Brock, R. The uptake of arginine-rich cell-penetrating peptides: putting the puzzle together. *Bioconjug. Chem.* **25**, 863-868 (2014).
35. Park, Y. J. *et al*. Nontoxic membrane translocation peptide from protamine, low molecular weight protamine (LMWP), for enhanced intracellular protein delivery: in vitro and in vivo study. *FASEB. J.* **19**, 1555-1557 (2005).
36. Li, Y. T. *et al*. Preliminary in vivo evaluation of the protein transduction domain-modified ATTEMPTS approach in enhancing asparaginase therapy. *J. Biomed. Mater. Res. A.* **91**, 209-220 (2009).
37. Ahn, S., Seo, E., Kim, K. & Lee, S. J. Controlled cellular uptake and drug efficacy of nanotherapeutics. *Sci. Rep.* **3**, 1997 (2013).
38. Cho, E. C., Xie, J., Wurm, P. A. & Xia, Y. Understanding the role of surface charges in cellular adsorption versus internalization by selectively removing gold nanoparticles on the cell surface with a I2/KI etchant. *Nano Letters* **9**, 1080-1084 (2009).
39. Pindiprolu, S., Chintamaneni, P. K., Krishnamurthy, P. T. & Ratna Sree Ganapathineedi, K. Formulation-optimization of solid lipid nanocarrier system of STAT3 inhibitor to improve its activity in triple negative breast cancer cells. *Drug Dev. Ind. Pharm.* 1-10 (2018).
40. dos Santos, T., Varela, J., Lynch, I., Salvati, A. & Dawson, K. A. Quantitative assessment of the comparative nanoparticle-uptake efficiency of a range of cell lines. *Small* **7**, 3341-3349 (2011).
41. Harush-Frenkel, O., Debotton, N., Benita, S. & Altschuler, Y. Targeting of nanoparticles to the clathrin-mediated endocytic pathway. *Biochem. Biophys. Res. Commun.* **353**, 26-32 (2007).
42. Verma, A. & Stellacci, F. Effect of surface properties on nanoparticle-cell interactions. *Small* **6**, 12-21 (2010).
43. Midoux, P. & Monsigny, M. Efficient gene transfer by histidylated polylysine/pDNA complexes. *Bioconjug. Chem.* **10**, 406-411 (1999).
44. Junghans, M., Kreuter, J. & Zimmer, A. Antisense delivery using protamine-oligonucleotide particles. *Nucleic Acids Res.* **28**, E45 (2000).
45. Harush-Frenkel, O., Rozentur, E., Benita, S. & Altschuler, Y. Surface charge of nanoparticles determines their endocytic and transcytotic pathway in polarized MDCK cells. *Biomacromolecules* **9**, 435-443 (2008).
46. Cu, Y., LeMoellic, C., Caplan, M. J. & Saltzman, W. M. Ligand-modified gene carriers increased uptake in target cells but reduced DNA release and transfection efficiency. *Nanomedicine* **6**, 334-343 (2010).
47. Verma, A. *et al*. Surface-structure-regulated cell-membrane penetration by monolayer-protected nanoparticles. *Nat. Mater.* **7**, 588-595 (2008).
48. Duchardt, F., Fotin-Mleczek, M., Schwarz, H., Fischer, R. & Brock, R. A comprehensive model for the cellular uptake of cationic cell-penetrating peptides. *Traffic* **8**, 848-866 (2007).
49. Park, Y. S. *et al*. Controlled release of simvastatin from in situ forming hydrogel triggers bone formation in MC3T3-E1 cells. *AAPS. J.* **15**, 367-376 (2013).